

# Morphometric Analysis Program and Quantitative Positron Emission Tomography in Presurgical Localization in MRI-negative Epilepsies: a Simultaneous PET/MRI Study

**Kun Guo**

Department of Radiology and Nuclear Medicine, Xuanwu Hospital Capital Medical University

**Jingjuan Wang**

Department of Radiology and Nuclear Medicine, Xuanwu Hospital Capital Medical University

**Zhenming Wang**

Department of Radiology and Nuclear Medicine, Xuanwu Hospital Capital Medical University

**Yihe Wang**

Department of Neurosurgery, Xuanwu Hospital Capital Medical University

**Bixiao Cui**

Department of Radiology and Nuclear Medicine, Xuanwu Hospital Capital Medical University

**Guoguang Zhao**

Department of Neurosurgery, Xuanwu Hospital Capital Medical University

**Jie Lu** (✉ [imaginglu@hotmail.com](mailto:imaginglu@hotmail.com))

Department of Radiology and Nuclear Medicine, Xuanwu Hospital Capital Medical University

<https://orcid.org/0000-0003-0425-3921>

---

## Research Article

**Keywords:** Epilepsy, PET/MRI, MAP, Quantitative PET, Localization

**Posted Date:** September 7th, 2021

**DOI:** <https://doi.org/10.21203/rs.3.rs-859735/v1>

**License:**  This work is licensed under a Creative Commons Attribution 4.0 International License.

[Read Full License](#)

---

**Version of Record:** A version of this preprint was published at European Journal of Nuclear Medicine and Molecular Imaging on December 23rd, 2021. See the published version at <https://doi.org/10.1007/s00259-021-05657-w>.

# Abstract

**Purpose:** To evaluate morphometric analysis program (MAP) and quantitative positron emission tomography (QPET) in epileptogenic zone (EZ) identification using a simultaneous positron emission tomography/magnetic resonance imaging (PET/MRI) system in MRI-negative epilepsies.

**Methods:** Seventy-one localization-related MRI-negative epilepsies underwent preoperative simultaneous PET/MRI examination and surgical resection were enrolled retrospectively. MAP was performed on T1-weighted volumetric sequence and QPET was analyzed using statistical parametric mapping (SPM) with comparison to age- and gender- matched normal controls. The sensitivity, specificity, positive predictive value (PPV) and negative predictive value (NPV) of MAP, QPET, MAP+ QPET and MAP/QPET in EZ localization were assessed. The correlations between surgical outcome and modalities concordant with cortical resection were analyzed.

**Results:** Forty-five (63.4%) patients had Engel I seizure outcome. The sensitivity, specificity, PPV and NPV of MAP was 64.4%, 69.2%, 78.3% and 52.9%, respectively. The sensitivity, specificity, PPV, NPV of QPET was 73.3%, 65.4%, 78.6%, and 58.6%, respectively. MAP+QPET, defined as two tests concordant with cortical resection, had reduced sensitivity (53.3%) but increased specificity (88.5%) relative to individual tests. MAP/QPET, defined as one or both tests concordant with cortical resection, had increased sensitivity (86.7%) but reduced specificity (46.2%) relative to individual tests. The regions determined by MAP, QPET, MAP+QPET or MAP/QPET concordant with cortical resection was significantly associated with seizure-free outcome, MAP+QPET performed best.

**Conclusion:** The combination of MAP and QPET imaging play a complementary role in EZ localization and this approach can be readily improved surgical outcome in MRI-negative epilepsies.

## Introduction

For the magnetic resonance imaging (MRI)-negative intractable focal epilepsy patients, identifying a subtle abnormality that was previously undetected helps to provide an opportunity for surgical treatment. Longitudinal studies in MRI-negative focal epilepsy patients showed that resected surgery offers the potential for long-term seizure control [1, 2], which encouraged researchers using postprocessing imaging analysis to identify more potential epileptogenic zone (EZ).

Morphometric analysis program (MAP), one of many MRI postprocessing imaging analysis, several researchers have demonstrated that MAP could be helped detect subtle abnormalities of focal cortical dysplasia (FCD) in MRI-negative surgical candidates [3–5]. However, the false-positive of MAP methodology caused by imaging artifacts, registration errors, and nonepileptic variants may lead to multiple regions on the output maps, which may resemble epileptogenic lesions. The focal hypometabolism foci shown on interictal  $^{18}\text{F}$ -fluorodeoxyglucose ( $^{18}\text{F}$ -FDG) positron emission tomography (PET) was associated with EZ [6, 7].  $^{18}\text{F}$ -FDG PET has been widely used in preoperative localization of drug-resistant epilepsy with a negative MRI [8, 9]. Quantitative PET (QPET) analysis using

statistical parametric mapping (SPM) can help to provide objective data, and improve the diagnostic of PET, especially in the patients with normal vision on PET scans [10–13]. There are fewer data in the literature on the sensitivity and specificity of combined post-processing imaging with localization-related MRI-negative epilepsies.

The combination of MAP and QPET imaging analysis facilitated objective identification of epileptogenic abnormalities have been reported by Lin. et al [14]. However, the non-simultaneous acquisition in different machines and times, various motion artifacts may lead to potential biases in the subtle EZ localization. In the present study, <sup>18</sup>F-FDG PET and MRI images were obtained from a simultaneous PET/MRI, the sensitivity, specificity, positive predictive value (PPV), and negative predictive value (NPV) of MAP, QPET, MAP + QPET, and MAP/QPET in detection EZ were evaluated. Moreover, whether the concordance between the regions identified by MAP and QPET and the surgical resection associated with seizure outcomes was explored.

## Material And Methods

### Patients and Healthy controls

This retrospective study was permitted by the Research Ethics Committee of the Capital Medical University of Xuanwu hospital. Written informed consent was obtained from each participant.

Patients were included if they had (1) MRI normal or subtle changes on an official neuroradiology report. (2) a preoperative simultaneous <sup>18</sup>F-FDG PET/MRI scan, (3) received a comprehensive presurgical evaluation included seizure semiology, video-electroencephalography (V-EEG), neuroimaging and intracranial EEG (IEEG) (4) postoperative follow-up of over 12 months, and (5) a postoperative MRI or CT scan. Patients were excluded if they had (1) poor PET/MRI quality hindering clinical read or (2) poor PET/MRI quality causing significant registration errors in the data processing procedures. None of the patients had intraoperative or perioperative complications, and the preoperative antiepileptic regimen was continued for all patients in the postoperative period.

Available microscopic slides from surgical resections were reviewed by a dedicated neuropathologist. Pathology results was classified according to the International League Against Epilepsy classification [15].

Seizure outcomes were categorized one-year after surgery by the Engel Epilepsy Surgery Outcome Scale. [16] Surgical outcome was then categorized as Engel I (seizure free) and Engel II-IV (non-seizure free). The demographic and clinical characteristics of all participants are presented in Table 1.

22 age- and gender-matched healthy controls (HCs) ((mean age, 29.32 ± 5.65 years, range, 17–39 years; 11 males) were enrolled. All HCs were free of psychiatric or neurologic disorders on the basis of a health screening measure.

## **PET/MRI acquisition**

Interictal  $^{18}\text{F}$ -FDG PET and MRI data were simultaneously obtained using a simultaneous TOF-PET/MR scanner (SIGNA, GE Healthcare, WI, USA). The patients fasted at least 6 hours, and the level of fasting blood glucose was lower than 11.1 mmol/L.  $^{18}\text{F}$ -FDG with radiochemical purity of > 95% was produced by the unit, and the injection dosage was calculated based on the patients' body weight (3.7 MBq/kg). All patients were at rest in a dimmed environment for 40 min. Video surveillance was used to monitor the patients in order to exclude an ictal or postictal FDG administration. During the scanning, the subjects were instructed to keep their eyes open, keep their head as still as possible. Three-dimension T1 brain volume imaging (3D T1 BRAVO) (repetition time (TR) = 2300ms, echo time (TE) = 2.98ms, angle = 9°, slices/gap = 160/0.5mm, FOV = 256mm, matrix size = 256×256, voxel size = 1.0×1.0×1.0mm<sup>3</sup>) and other structural imaging sequences for diagnosis images were immediately obtained.

The PET bed position included a simultaneous 18-second 2-point Dixon scan for MRI. Attenuation correction, scatter correction, random correction, and dead-time correction were also performed. Scanning parameters for reconstructed images were as follows: matrix size = 192×192, voxel size = 1.82×1.82×2.78 mm<sup>3</sup>, 89 slices. PET image reconstruction with ordered subset expectation maximization algorithm (OSEM) 3 iterations, and 32 subsets, time-of flight and Sharp IR.

## **MRI postprocessing**

MAP was performed on 3D T1 BRAVO images using an in-house code in MATLAB. The computed output consists of 3 volumetric statistical maps, called the junction, extension, and thickness maps. A blinded reviewer used the z score threshold of 4 to identify candidate MAP positive regions on the junction file, an accompanying region on the extension file ( $z > 6$ ) and the thickness file ( $z > 4$ ). The choice of z score threshold was consistent with previous literature [3]. Candidate MAP positive regions were searched in the whole brain. All candidate MAP positive regions were then addressed by two experienced neuroradiologists, who conducted a corresponding focused re-review of the preoperative clinical MRI (with 3D T1 BRAVO, T2-weighted FLAIR, and turbo spin echo sequences), if they have any opinions, a third neuroradiologists needed to determine. The MAP result was classified as concordant with cortical resection if the abnormal area included the resection site; otherwise, it was classified as non-concordant with cortical resection.

## **QPET analysis**

All imaging data were preprocessed in SPM12 (<http://www.fil.ion.ucl.ac.uk/spm/software/spm12>) and an in-house code in MATLAB. Glucose metabolism from all HCs were served as the normal databases. To assess the individual glucose metabolism changes, a two-sample t-test was performed between individual patient data and normal database, with age and gender regressed out as covariates to reduce the effects of these variables. Global nuisance effects were estimated by dividing the intensity in each image by the intensity of the cerebellum. Registered PET maps were spatially normalized to the Montreal Neurological Institute (MNI) space by the same transformation parameters from the segmentation

procedure of the T1-weighted images. Preprocessed PET images in MNI space were converted to the standardized uptake value ratio (SUVr) relative to the cerebellum and then smoothed using a 6-mm full width at half maximum (FWHM) Gaussian kernel. The resulting SPM (t) maps were thresholded with a significance level of  $P < 0.05$  without corrections. The SPM (t) maps reviewed by a dedicated nuclear medicine physician to exclude the focal metabolism caused by sulcus, if the physician has any questions, another physician is required to make a decision after consultation. The QPET result was interpreted as a normal or abnormal scan. If the SPM (t) maps was abnormal, the anatomic location of abnormal metabolism was recorded. The QPET result was classified as concordant with cortical resection if the abnormal metabolic area included the resection area; otherwise, it was classified as non-concordant with cortical resection.

For the combined MAP + QPET, if the results of both of the tests were concordant with cortical resection, the combined tests were considered as concordant; conversely, if the result of one of the tests was non-concordant, the combined tests were considered as non-concordant. For MAP/QPET, if the result of one of the tests were concordant, the tests were considered as concordant; conversely, MAP/QPET was considered non-concordant if both tests were non-concordant.

## Statistical analysis

All data analysis was performed with SPSS software (IBM SPSS Statistics, Version 21.0). Group-level comparisons of demographic and clinical characteristics were carried out with independent-sample Student's t-tests, one-way analysis of variance, or chi-square tests.  $P < 0.05$  was considered statistically significant. True positive (TP) was classified as if the imaging results concordant with surgical resection in seizure-free patients (Engel I), imaging results non-concordant with surgical resection in patients with ongoing seizures (Engel II-IV) was classified as false positive (FP). The imaging results non-concordant with surgical resection in patients with ongoing seizures was classified as true negative (TN). Such a case neuroimaging found no focal lesion and surgery proceeded, but the patient did not improve. False negative (FN) was defined as imaging results concordant with the actual surgical resection in seizure-free patients. Sensitivity =  $TP / (TP + FN)$ , Specificity =  $TN / (TN + FP)$ , PPV =  $TP / (TP + FP)$ , NPV =  $TN / (TN + FN)$ . Associations between the regions identified by QPET and MAP concordant with cortical resection and seizure outcome at least one-year were tested by Chi-square tests.

# Results

## Subjects

Seventy-one epilepsy patients with a negative MRI were included. There was no significant difference between the epilepsy patients and healthy controls in age or gender ( $P > 0.05$ ). Forty-five (63.4%) patients had Engel I seizure outcome at one-year follow-up. There was no significantly different between the seizure-free (Engel I) and non-seizure-free (Engel II-IV) groups in other clinical characteristics including age of onset, epilepsy duration, history of medication and resection area ( $P > 0.05$ ). The detailed demographics and clinical data of patients and healthy controls were listed in Table 1.

Surgical pathology included FCD in 48 (67.6%) patients (including FCD I in 36 cases, FCD II in 9 cases and FCD III in 3 cases), HS in 5 (7.0%) patients, FCD associated with HS in 3 (4.2%) patients, and other pathology in 3 (4.2%) patients (ulegyria in 2 patients and ganglioglioma WHO I in one patient). 12 (16.9%) patients had negative surgical histology.

## MAP

Candidate MAP positive regions were found in 50 patients (70.4%), including 35 patients with single candidate MAP positive regions and 15 patients with multiple candidate MAP positive regions. Candidate MAP positive regions was concordant with cortical resection in 37 patients, of whom 29 patients achieved Engel I seizure outcome and eight patients with Engel II-IV seizure outcome. MAP was negative in 21 patients, and localized but non-concordant with cortical resection in 13 patients, of whom 16 patients achieved Engel I seizure outcome and 18 patients with Engel II-IV seizure outcome. The sensitivity of MAP was 64.40%, specificity was 69.2%, PPV was 78.3%, and NPV was 52.9% (Table 2). Candidate MAP positive regions concordant with cortical resection was associated with favorable seizure outcomes ( $P= 0.006$ ) (Table 3).

## QPET

QPET positive regions were found in 66 patients (93.0%), including 56 patients with single site hypometabolism and 10 patients with multiple site hypometabolism. QPET positive regions was concordant with surgical resection in 42 patients, among them, 33 patients achieved Engel I seizure outcome and nine patients with Engel II-IV seizure outcome. QPET found no apparent hypometabolism in five patients, and localized but non-concordant with surgical resection in 29 patients, of whom 12 patients achieved Engel I seizure outcome and 17 patients with Engel II-IV seizure outcome. The sensitivity of QPET was 73.30%, specificity was 65.4%, PPV was 78.6%, and NPV was 58.6% (Table 2). The region determined by QPET concordant with surgical resection was associated with favorable seizure outcomes compared to the ones non-concordant with surgical resection ( $P= 0.001$ ) (Table 3). There was a significant difference between MAP and QPET for concordance with cortical resection ( $\chi^2 = 4.79$ ,  $P= 0.029$ ). (Table 4). Figure 1 shows four representative cases with presurgical imaging evaluation and postsurgical CT.

## MAP + QPET

The regions located by the combination of MAP + QPET concordant with surgical resection in 27 patients, among them, 24 patients achieved Engel I surgical outcome and three patients still with ongoing seizures. One or both of the combined tests were non-concordant with the surgical resection in 21 patients with Engel I seizure outcome, and in 23 patients with Engel II-IV seizure outcome. The sensitivity of MAP + QPET was 53.3%, specificity was 88.5%, PPV was 88.9%, and NPV was 52.3% (Fig. 2). The region determined by MAP + QPET concordant with surgical resection was associated with favorable seizure outcomes compared to the ones non-concordant with cortical resection ( $P < 0.001$ ) (Table 3).

## MAP/QPET

The MAP/QPET was concordant with cortical resection in 39 patients with Engel I surgical outcome, and 14 patients with Engel II-IV surgical outcome. The regions located by the combination of MAP/QPET non-concordant with surgical resection in 18 patients, among them, six patients achieved Engel I surgical outcome and 12 patients still with ongoing seizures. The sensitivity of MAP/QPET was 86.7%, specificity was 46.2%, PPV was 73.6%, and NPV was 66.6% (Fig. 2). The region determined by MAP/QPET concordant with surgical resection was associated with favorable seizure outcomes compared to the ones non-concordant with cortical resection ( $P=0.002$ ) (Table 3). The correlation between surgical outcome and MAP or QPET localization results were shown in Fig. 3.

## Discussion

We calculated sensitivity, specificity, PPV, and NPV of MAP and QPET in patients with Engel I seizure outcome following cortical resection and assessed the association between localization of diagnostic test relative to cortical resection and surgical outcomes. The sensitivity, specificity, PPV, and NPV of MAP were 64.4%, 69.2%, 78.3% and 52.9%, respectively. The sensitivity, specificity, PPV, and NPV of QPET were 73.3%, 65.4%, 78.6%, and 58.6%, respectively. The combined MAP + QPET have lower sensitivity (53.3%) and higher specificity (88.5%) relative to individual diagnostic tests. When used for the two tests MAP/QPET, the sensitivity increased (86.7%) and the specificity (46.2%) decreased relative to individual diagnostic tests. Whether MAP or QPET, concordant with cortical resection both associated with favorable surgical outcome when compared to non-concordant with cortical resection, MAP + QPET performed best.

MAP is increasingly used to complement visual analysis and elucidate structural epileptogenic lesions in preoperative evaluation. Wang et al. performed a retrospective study in 150 “non-lesional” epilepsies patients and shown that MAP positive areas were detectable in 65 patients (43%) [3]. Lin et al. showed MAP positive regions were found in 82 of the 104 patients (79%) [14]. Our retrospective study detected candidate MAP positive regions in 70.4% (50/71) patients. Setting the cortical resection and surgical outcome as criterion, the sensitivity and specificity was 64.40% and 69.2% for Engel I surgical outcome. The differences in detection rates may be explained by non-uniform inclusion criteria of MRI negative patients. The absence of a lesion on MRI has consistently been shown as a predictor for surgical failure [17, 18]. MAP results turned some cases from MRI negative to MRI positive, these patients are more likely to become seizure free following cortical resection of the subtle lesion. Previous studies shown complete resection of the MAP positive region correlated positively with seizure-free outcome [3, 5, 14]. Our study also found that MAP positive regions concordant with cortical resection associated with a favorable surgical outcome compared to the non-concordant ones. Those results indicated that MAP positive region may be a potential epileptogenic lesion, since MAP is only a postprocessing method without incurring any additional cost or risk to patients, may be applied to standard preoperative evaluation.

Although previous studies demonstrated visual analysis yielded similar findings to SPM analysis of abnormal metabolism in localization-related epilepsy [13, 19], a quantitative analysis may be more subjective and identify more areas of abnormal metabolism. Tomás et al shown QPET sensitivity and specificity were both 95% in temporal lobe epilepsy (TLE) patients and 80% and 95% respectively in extratemporal epilepsy (ETLE) patients in a study including 130 epilepsy patients [20]. Lin et al. evaluated QPET thresholds of standard deviations (SDs) of -1, -2, -3, and -4 to identify the optimal threshold for QPET analysis, and they demonstrated that the QPET SD threshold of +2 showed the best combination of positive rate (55%), sensitivity (68%) and specificity (88%) [14]. In this study,  $P < 0.05$  without correction for multiple comparisons was considered statistically significant in  $^{18}\text{F}$ -FDG PET images processed. Since at the beginning we have performed 2 thresholds ( $P < 0.05$ ;  $P < 0.01$ ) for multiple comparisons, however, near 30% patient shown no apparent hypometabolism on SPM (t) maps for  $P < 0.01$  without correction. The sensitivity (73.3%) was similar with previous study. The specificity (65.4%) was lower, the specificity was extremely limited in the retrospective study that QPET did not guide surgical resections. Lin et al. found that when PET is used alone, lobar localization yielded by visual PET analysis or QPET was not associated with seizure-free outcome [14]. As the areas of hypometabolism shown on PET often extending beyond the epileptogenic region, PET is best suited for lobar localization of the potentially epileptogenic region rather than as a precise determination of surgical margins. Our study found that QPET regions concordant with cortical resection associated with a favorable surgical outcome, because the classification in our study defined the concordant was whether the abnormal metabolic area included the resection area.

The combined MAP + QPET increased the specificity of the tests and therefore reduced the number of false-positive tests, whereas the MAP/QPET tests increased the sensitivity and therefore reduced the number of false-negative tests for Engel I surgical outcome. Similar with other multimodality imaging studies [21], although they chose different modalities, all indicated that if one diagnostic test was non-localizing, a second diagnostic test could increase the likelihood of localizing the epileptogenic zone. Ding et al. [22] shown that presurgical evaluation by co-registration of  $^{18}\text{F}$ -FDG PET and MRI could improve the identification of the epileptogenic onset zone, and may further guide surgical and improve the outcome in the refractory ETLE patients with normal MRI. Desarnaud et al. [23] integrated electroclinical data and PET/MRI co-registration, and obtained a high localizing value of 83% in FCD patients. Lin et al. [14] utilized QPET analysis to complement MAP to facilitate automated identification of subtle FCD, reveals the usefulness of QPET-MAP analysis in detecting potentially epileptogenic lesions and find the association between the resection of the QPET-MAP positive regions and good seizure outcome. In the present study, the PET and MRI images in our study was obtained from a simultaneous PET/MRI scanner, whether MAP + QPET or MAP/QPET, the abnormalities concordant with cortical resection was significantly associated with seizure-free outcomes, MAP + QPET performed better. MAP shown multiple candidate regions, QPET could help excluding those candidate MAP positive regions caused by imaging artifacts, registration errors, or nonepileptic variants. The broader localization of QPET is complemented by the more precise localization of potential structural abnormalities identified by MAP. Mendes Coelho et al. [24] demonstrated QPET had critical value for patients with subtle MRI findings.

Another study also shown combined features assisted by machine learning from MRI and PET outperformed in FCD localization [25]. Those published studies along with our results suggest that correlating findings from functional and structural methods improve the identification of EZ and surgical outcomes.

The main limitation that this was a retrospective study, many confounding factors may be affected surgery outcome, the patients who actually benefitted from a workflow reduction may be not calculated. Secondly, the comprehensive preoperative evaluation also includes symptomatology, intracardial EEG, etc, the QPET and MAP results may be not direct surgical resection, so the specificity of diagnostic tests in epileptic foci localization may be limited. Thirdly, simultaneous review of the MR and PET images was also an advantage of simultaneous PET/MRI, however, the image interpretation was read separately.

## Conclusions

In conclusion, the combination of QPET and MAP imaging obtained from a simultaneous PET/MRI scanner play a complementary role in detection EZ for preoperative evaluation in MRI-negative epilepsies. The combined MAP+QPET can improve the specificity of the diagnostic tests, whereas MAP/QPET can increase the sensitivity of the diagnostic tests.

## Declarations

**Funding:** This work was supported by the Beijing Municipal Administration of Hospitals Ascent Plan [grant number DFL20180802].

**Conflicts of interest/Competing interests:** The authors declare that they have no conflict of interest.

**Availability of data and material:** Data and materials are available from Jie Lu.

**Research involving human participants and/or animals:** The research involved human participants. This retrospective study was permitted by the Research Ethics Committee of the Capital Medical University of Xuanwu hospital.

**Consent to participate:** All patients gave written informed consent prior to enrollment in this study.

**Acknowledgments:** We thank Yuchao Xu, PHD and Yan Guo, MD from GE Healthare for editing drafts and statistical suggestions of this manuscript.

## References

1. Malmgren K, Krýsl D. [Epilepsy: Long-term outcomes in MRI-negative patients with epilepsy](#). *Nat Rev Neurol*. 2017;13:132-3.
2. Pellinen J, Kuzniecky R, Doyle W, Devinsky O, Dugan P. MRI-negative PET-negative epilepsy long-term surgical outcomes: A single-institution retrospective review. *Epilepsy Res*. 2020; 67:106481.

3. Wang ZI, Jones SE, Jaisani Z, Najm IM, Prayson RA, Burgess RC, et al. Voxel-based morphometric magnetic resonance imaging (MRI) postprocessing in MRI-negative epilepsies. *Ann Neurol.* 2015; 77:1060-75.
4. Sun K, Ren Z, Yang D, Wang X, Yu T, Ni D, et al. Voxel-based morphometric MRI post-processing and PET/MRI co-registration reveal subtle abnormalities in cingulate epilepsy. *Epilepsy Res.* 2021; 171:106568.
5. Wagner J, Weber B, Urbach H, Elger CE, Huppertz HJ. Morphometric MRI analysis improves detection of focal cortical dysplasia type II. *Brain.* 2011; 134:2844-54.
6. Kim YK, Lee DS, Lee SK, Kim SK, Chung CK, Chang KH, et al. Differential features of metabolic abnormalities between medial and lateral temporal lobe epilepsy: quantitative analysis of (18)F-FDG PET using SPM. *J Nucl Med.* 2003; 44:1006-12.
7. Liu F, Ruan W, Deng X, Song Y, Song W, Hu F, et al. Efficacy of delayed <sup>18</sup>F-FDG hybrid PET/MRI for epileptic focus identification: a prospective cohort study. *Eur J Nucl Med Mol Imaging.* 2021; 48:293-301.
8. Zhu Y, Feng J, Wu S, Hou H, Ji J, Zhang K, et al. Glucose metabolic profile by visual assessment combined with statistical parametric mapping analysis in pediatric patients with epilepsy. *J Nucl Med.* 2017; 58:1293-9.
9. von Oertzen TJ. PET and ictal SPECT can be helpful for localizing epileptic foci. *Curr Opin Neurol.* 2018; 31:184-91.
10. Ponisio MR, Zempel JM, Day BK, Eisenman LN, Miller-Thomas MM, Smyth MD, et al. The Role of SPECT and PET in Epilepsy. *AJR Am J Roentgenol.* 2021; 216:759-68.
11. Mayoral M, Marti-Fuster B, Carreño M, Carrasco JL, Bargalló N, Donaire A, et al. Seizure-onset zone localization by statistical parametric mapping in visually normal (18) F-FDG PET studies. *Epilepsia.* 2016; 57:1236-44.
12. Peter J, Houshmand S, Werner TJ, Rubello D, Alavi A. Applications of global quantitative 18F-FDG-PET analysis in temporal lobe epilepsy. *Nucl Med Commun.* 2016; 37:223-30.
13. Kumar A, Juhász C, Asano E, Sood S, Muzik O, Chugani HT. Objective detection of epileptic foci by <sup>18</sup>F-FDG PET in children undergoing epilepsy surgery. *J Nucl Med.* 2010; 51:1901-7.
14. Lin Y, Fang YD, Wu G, Jones SE, Prayson RA, Moosa ANV, et al. Quantitative positron emission tomography-guided magnetic resonance imaging postprocessing in magnetic resonance imaging-negative epilepsies. *Epilepsia.* 2018; 59:1583-94.
15. Blümcke I, Thom M, Aronica E, Armstrong DD, Vinters HV, Palmini A, et al. The clinicopathologic spectrum of focal cortical dysplasias: a consensus classification proposed by an ad hoc Task Force of the ILAE Diagnostic Methods Commission. *Epilepsia.* 2011; 52:158-74.
16. Engel JJ, Van Ness NP, Rasmussen TB, Ojemann LM. Outcome with respect to epileptic seizures. In: Engel JJ, ed. *Surgical treatment of the epilepsies.* 2nd ed. New York, NY: Raven Press, 1993; 609-21.
17. Ryvlin P, Rheims S. [Predicting epilepsy surgery outcome.](#) *Curr Opin Neurol.* 2016; 29:182-8.

18. Krucoff MO, Chan AY, Harward SC, Rahimpour S, Rolston JD, Muh C, et al. Rates and predictors of success and failure in repeat epilepsy surgery: A meta-analysis and systematic review. *Epilepsia*. 2017; 58:2133-42.
19. Juhász C, John F. Utility of MRI, PET, and ictal SPECT in presurgical evaluation of non-lesional pediatric epilepsy. *Seizure*. 2020; 77:15-28.
20. Tomás J, Pittau F, Hammers A, Bouvard S, Picard F, Vargas MI, et al. The predictive value of hypometabolism in focal epilepsy: a prospective study in surgical candidates. *Eur J Nucl Med Mol Imaging*. 2019; 46:1806-16.
21. Widjaja E, Shamma A, Vali R, Otsubo H, Ochi A, Snead OC, et al. FDG-PET and magnetoencephalography in presurgical workup of children with localization-related non-lesional epilepsy. *Epilepsia*. 2013; 54:691-9.
22. Ding Y, Zhu Y, Jiang B, Zhou Y, Jin B, Hou H, et al. <sup>18</sup>F-FDG PET and high-resolution MRI co-registration for pre-surgical evaluation of patients with conventional MRI-negative refractory extra-temporal lobe epilepsy. *Eur J Nucl Med Mol Imaging*. 2018; 45:1567-72.
23. Desarnaud S, Mellerio C, Semah F, Laurent A, Landre E, Devaux B, et al. <sup>18</sup>F-FDG PET in drug-resistant epilepsy due to focal cortical dysplasia type 2: additional value of electroclinical data and co-registration with MRI. *Eur J Nucl Med Mol Imaging*. 2018; 45:1449-60.
24. Mendes Coelho VC, Morita ME, Amorim BJ, Ramos CD, Yasuda CL, Tedeschi H, et al. Automated online quantification method for <sup>18</sup>F-FDG positron emission tomography/CT improves detection of the epileptogenic zone in patients with pharmaco-resistant epilepsy. *Front Neurol*. 2017; 8:453.
25. Tan YL, Kim H, Lee S, Tihan T, Ver Hoef L, Mueller SG, et al. Quantitative surface analysis of combined MRI and PET enhances detection of focal cortical dysplasia. *Neuroimage*. 2018; 166:10-8.

## Tables

Table 1

Detailed demographics and clinical data of patients

<b>Variable</b>	<b>Total</b> (n=71)	<b>Seizure-free</b> (n=45)	<b>Non-seizure-free</b> (n=26)	<b>P</b>
<b>Gender</b> (n, %)				0.14 <sup>b</sup>
Male	44 (62.0)	25 (55.6)	19 (73.1)	
Female	27 (38.0)	20 (44.4)	7 (26.9)	
<b>Age</b> (y, mean±SD)	25.7±9.4	26.0±9.3	25.3±9.6	0.79 <sup>a</sup>
<b>Age group</b>				0.49 <sup>b</sup>
≥18y	57 (80.3)	35 (77.8)	22 (84.6)	
<18y	14 (19.7)	10 (22.2)	4 (15.4)	
<b>Age of onset</b> (y, mean±SD)	13.3±8.6	13.5±8.3	13.0±9.2	0.83 <sup>a</sup>
<b>Duration</b> (y, mean±SD)	12.3±8.4	12.4±8.7	12.1±8.2	0.88 <sup>a</sup>
<b>Febrile convulsion</b> (n, %)	9 (12.7)	6 (13.3)	3 (11.5)	0.83 <sup>b</sup>
<b>Medication</b> (n, %)				0.72 <sup>b</sup>
≤ 2	39(54.9)	24 (53.3)	15 (57.7)	
>2	32(45.1)	21 (46.7)	11 (42.3)	
<b>Resection area</b> (n, %)				0.33 <sup>b</sup>
Frontal	13 (18.3)	10 (22.2)	3 (11.5)	
Parietal	7 (9.9)	3 (6.7)	4 (15.4)	
Occipital	1 (1.4)	0 (0)	1 (3.8)	
Temporal	39 (54.9)	26 (57.8)	13 (50)	
Multi-lobar	11 (15.5)	6 (13.3)	5 (19.2)	

SD, standard deviation.

<sup>a</sup> t test. <sup>b</sup> Pearson chi-square test.

Table 2

Sensitivity, specificity, positive predictive value (PPV), and negative predictive value (NPV) of lobar localization of MAP, QPET, MAP+QPET, and MAP/QPET for Engel I seizure outcome

	<b>Sensitivity</b>	<b>Specificity</b>	<b>PPV</b>	<b>NPV</b>
<b>MAP</b>	<b>64.4%</b>	<b>69.2%</b>	<b>78.3%</b>	<b>52.9%</b>
(95% CI)	(0.49-0.78)	(0.48-0.86)	(0.62-0.90)	(0.35-0.70)
<b>QPET</b>	<b>73.3%</b>	<b>65.4%</b>	<b>78.6%</b>	<b>58.6%</b>
(95% CI)	(0.58-0.85)	(0.44-0.83)	(0.63-0.90)	(0.39-0.76)
<b>MAP+QPET</b>	<b>53.3%</b>	<b>88.5%</b>	<b>88.9%</b>	<b>52.3%</b>
(95% CI)	(0.38-0.68)	(0.70-0.98)	(0.71-0.98)	(0.37-0.68)
<b>MAP/QPET</b>	<b>86.7%</b>	<b>46.2%</b>	<b>73.6%</b>	<b>66.6%</b>
(95% CI)	(0.73-0.95)	(0.27-0.67)	(0.60-0.85)	(0.41-0.87)

CI, confidence interval; PPV, positive predictive value; NPV, negative predictive value.

Table 3

Correlation analysis between surgical outcome and MAP, QPET, MAP+QPET, MAP/QPET concordant or non-concordant with cortical resection

	<b>Engel I</b>	<b>Engel II-IV</b>	<b>P</b>
	<b>(n=45)</b>	<b>(n=26)</b>	
<b>MAP</b>			<b>0.006**</b>
Concordant with resection	29	8	
Non-concordant with resection	16	18	
<b>QPET</b>			<b>0.001**</b>
Concordant with resection	33	9	
Non-concordant with resection	12	17	
<b>MAP+QPET</b>			<b>0.001***</b>
Concordant with resection	24	3	
Non-concordant with resection	21	23	
<b>MAP/QPET</b>			<b>0.002**</b>
Concordant with resection	39	14	
Non-concordant with resection	6	12	

$P$  was test by chi-square test, \*\* $P < 0.01$ , \*\*\*  $P < 0.001$ .

Table 4

The difference between MAP and QPET for concordance with cortical resection

		QPET		$\chi^2$	$P$
		Concordant	Non-concordant		
MAP	Concordant	27	11	4.70	0.029*
	Non-concordant	15	18		

$P$  was test by chi-square test. \*  $P < 0.05$ .

## Figures

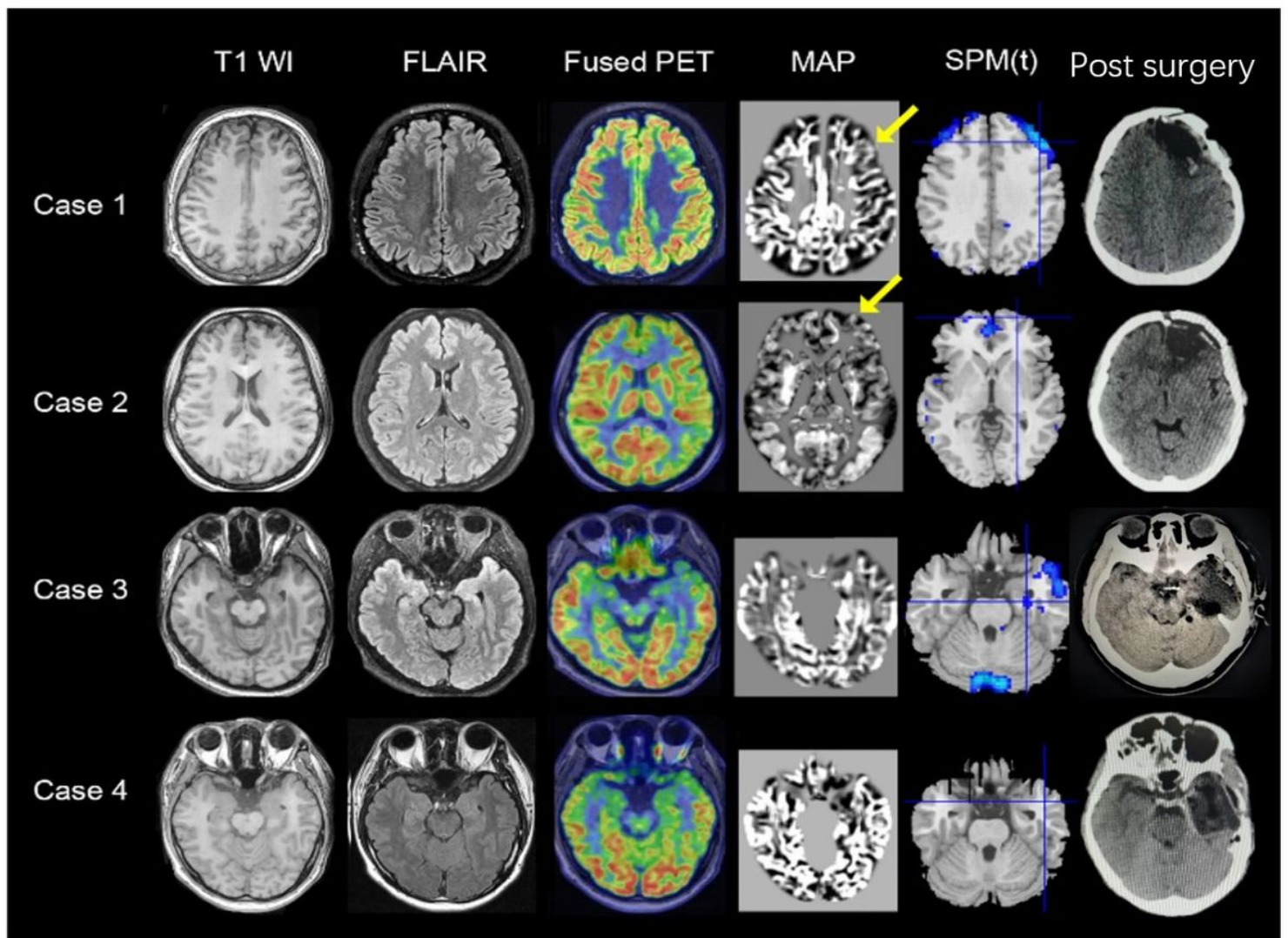


Figure 1

Examples of four patients with QPET and MAP results and surgical resection. Case 1, QPET and MAP indicated the region in the left frontal lobe, the patients achieved seizure-free at one year; Case 2, QPET shown no definitively hypometabolism, and MAP indicated the region in the left frontal lobe, the patients achieved seizure-free at one year. Case 3, QPET shown hypometabolism in the left temporal lobe and hippocampus, and MAP was negative, the patients achieved seizure-free at one year. Case 4, both QPET and MAP was negative, surgical resection was performed on the left temporal lobe based on other preoperative evaluation, the patient was Engel III at one-year.

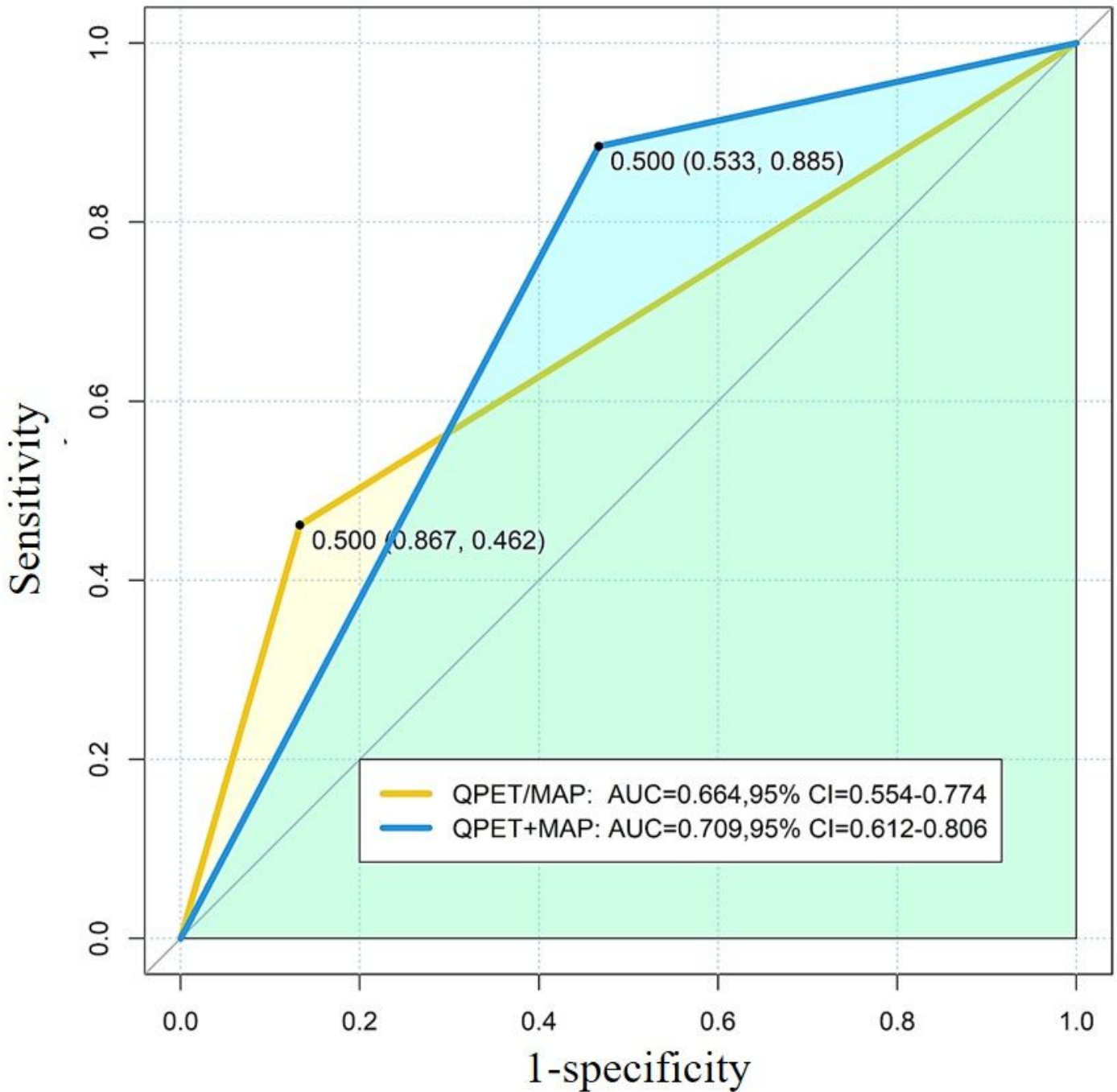
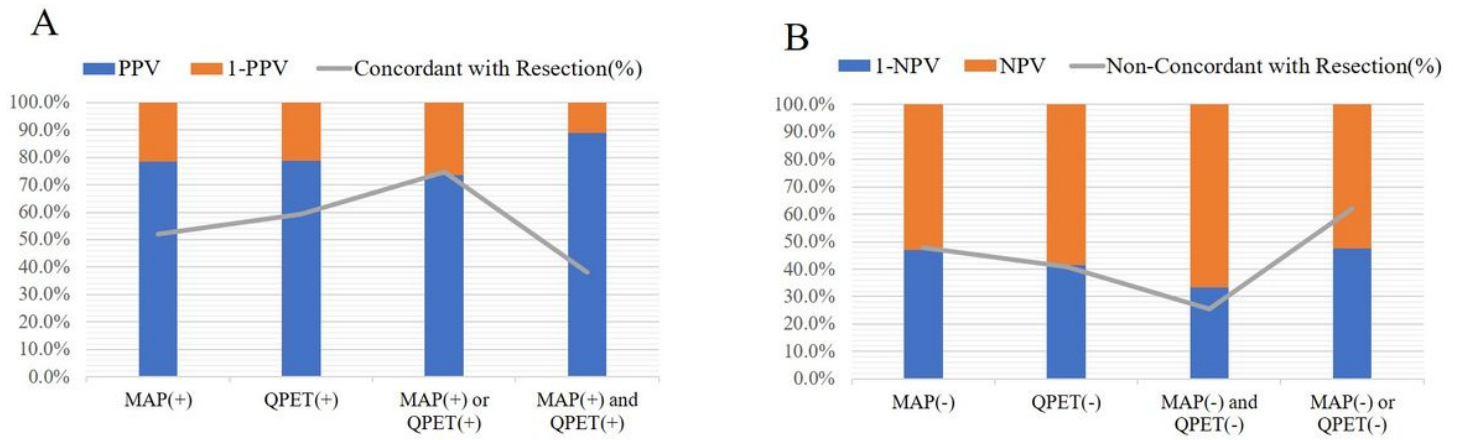


Figure 2

The ROC curves of MAP+QPET and MAP/QPET. For the combination of MAP/QPET, defined as one or both test(s) concordant with surgical resection, had increased sensitivity but reduced specificity relative to individual tests, the area under curve was 0.664, 95% CI (0.554-0.774). For the combination of MAP+QPET, defined as two tests concordant with surgical resection, had reduced sensitivity but increased specificity relative to individual tests, the area under curve was 0.709, 95% CI (0.612-0.806).



**Figure 3**

Correction between surgical outcome and MAP or QPET localization results. The regions located by the combination of MAP+QPET concordant with surgical resection in 27 patients, among them, 88.9% patients achieved Engel I surgical outcome. However, the positive ratio of QPET (+) and MAP (+) was only 38.0%; For 18 patients with MAP (-) and QPET (-), but surgery still performed, 66.7% were Engel II-IV at one-year follow-up.